Nanocomposite Metallic Thin Films for MEMS and NEMS Applications

[1*]V. Radmilovic, [1]Z. Lee, [2]C. Ophus, [2]E. Luber, [2]D. Mitlin and [1]U. Dahmen

[1]National Center for Electron Microscopy, LBNL, One Cyclotron Rd., Berkeley, CA 94720

[2]Department of Materials and Chemical Eng., University of Alberta, Canada

Introduction

Although silicon has low ductility and wear resistance, poor fracture toughness, electrical conductivity and optical reflectivity, it has been widely used in fabrication of micro–electromechanical / nano–electromechanical systems MEMS / NEMS [1]. Nanocomposite thin films have been proposed as a potential substitute for Si in MEMS/NEMS device applications since metals offer higher electrical conductivity and superior ductility [2]. However, polycrystalline metallic films typically exhibit low strength and hardness, high surface roughness, and significant residual stress. In this study we investigated the structure and properties of nanocomposite (Mo rich nanocrystals in Al-based and Ni-based amorphous matrices) Al-Mo and Ni-Mo binary alloy thin films.

Experimental

Al-Mo films of nominal compositions ranging from pure Al or Ni to films with 50at%Mo were produced by DC magnetron co-sputtering from pure Mo and pure Al and Ni targets. All films had a thickness in the range of 1.5-2.0 μm.
The resistivity of the films was measured using a standard thin film four-point probe test. Mechanical properties were assessed with a commercially available nanoindentation load-depth sensing instrument, and the film surface roughness was obtained using a tapping mode AFM probe. Conventional TEM was performed in a JEOL 200CX microscope at 200 kV. High resolution imaging was performed at 200 kV in a Philips CM200-FEG TEM and at 150 kV in a Philips CM300-FEG TEM.

Results and Discussion

Fig. 1 shows SEM images of Al-Mo grain structures for different alloy compositions. The pure Al films show a bimodal grain size distribution, which is often observed in pure fcc metallic films. The Al-8at.%Mo samples show a much finer surface structure. The Al-32at.%Mo films possess virtually featureless surfaces at the displayed magnification. The Al-55at.% films display mostly faceted crystallographic surfaces.

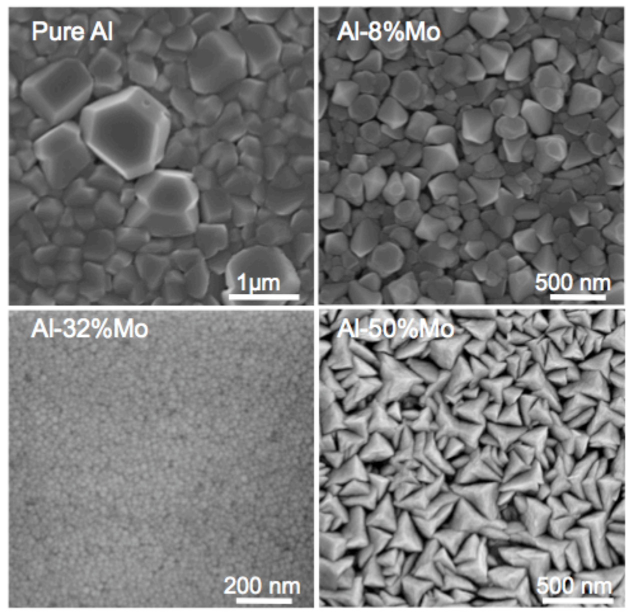

Fig. 1 SEM images of Al-Mo grain structures.

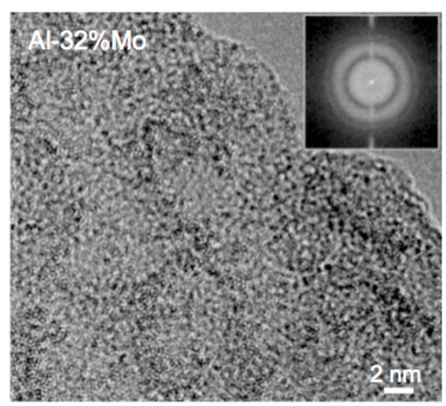

Fig. 2 HRTEM image of Al-Mo films in cross section.

The high resolution TEM image in Fig. 2 confirms the nanocomposite nature of the Al-32%Mo film.
The optimum film composition of Al-32at%Mo exhibits a unique microstructure comprised of a dense distribution of nm-scale Mo crystallites

dispersed in an amorphous Al-rich matrix. As seen from the measurements in Fig. 3, these films were found to have unusually high nanoindentation hardness and a very significant reduction in roughness compared to pure Al, while maintaining resistivity in the metallic range.

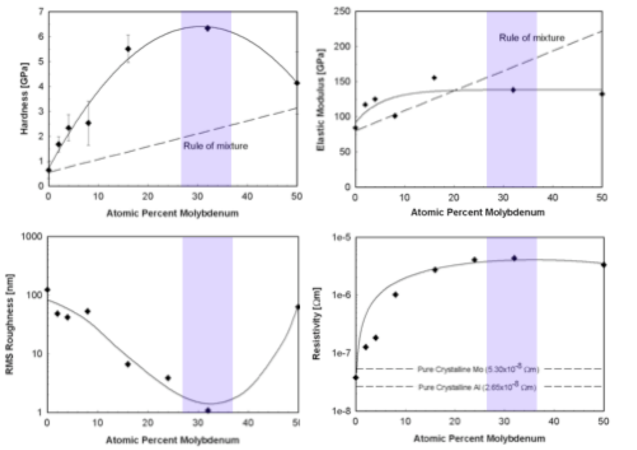

Fig. 3 Properties of Al-Mo thin films.

Fig. 4 shows SEM images of Ni-Mo grain structures. Similar to Al, the pure Ni films show a bimodal grain size distribution. The Ni-23at.%Mo samples are still fully crystalline with lower surface roughness. The Ni-44at.%Mo films possess very low surface roughness, around 1 nm. The Ni-87at.% films display mostly faceted crystallographic surfaces. An optimum structure and composition was achieved for Al-44at. %Mo exhibiting exceptional nanoindentation hardness, very low roughness and tunable internal stresses (Fig. 5). Using a sub-regular solution model we demonstrate that the electrical conductivity of Ni-Mo is in excellent agreement with Bhatia's structural model [3] of electrical resistivity in binary alloys.

Conclusion

By careful control of processing parameters, optimum microstructures in both Al-32at%Mo and Ni-44at.%Mo are obtained, consisting of nanocrystalline Mo islands densely and randomly dispersed in an amorphous Al-rich and Ni-rich matrices. Both films exhibit high nanoindentation hardness, metallic conductivity, and the surfaces display smooth morphology characteristic of sputtered amorphous films. Al-Mo films possess tunable residual stresses.

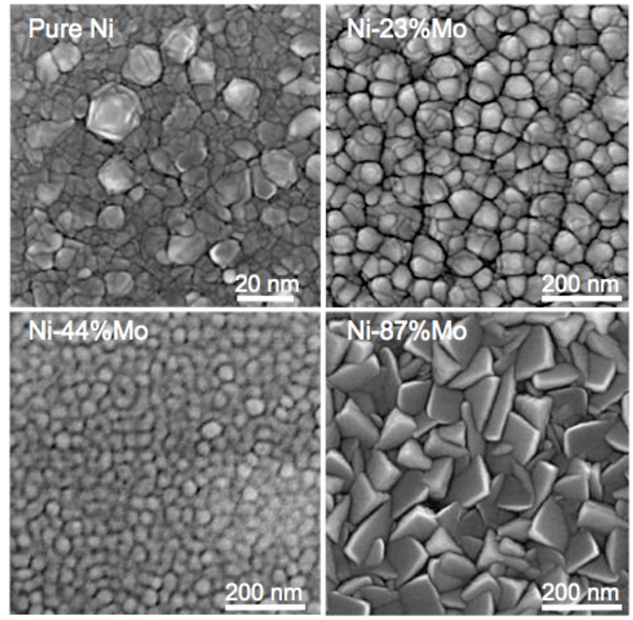

Fig. 4 SEM images of Ni-Mo grain structures.

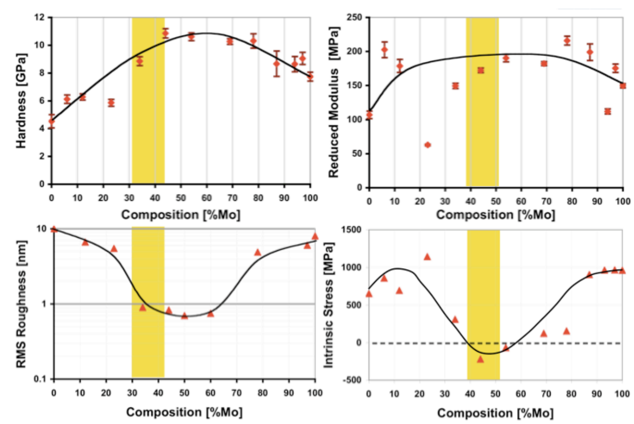

Fig. 5 Properties of Ni-Mo thin films.

References

1. A. Folch et al., *J. Microelectromech. Syst.,* **6** (1997) 303-306.
2. Z. Lee, et al., *Nanotechnology*, **17** (2006) 3063–3070.
3. A.B. Bhatia and D.E. Thornton, *Phys. Rev. B,* **2** (1970) 3004-3012.

This work was supported by the Director, Office of Energy Research, Office of Basic Energy Sciences, Materials Sciences Division, U. S. Department of Energy under Contract # DE-AC02-05CH11231 and Natural Science and Engineering Research Council of Canada (NSERC) Discovery Grant.
*VRRadmilovic@lbl.gov